Physical wellbore model for investigating the skin effect on the wellbore and its surroundings

Václav Ficaj [1], Pavel Pech [1], Daniel Kahuda [1] and Jan Kukačka [1,2]

[1] Faculty of Environmental Sciences, Czech University of Life Sciences Prague, Kamýcká 129, Prague – Suchdol, 165 00, Czech Republic
[2] Dekonta, a.s., Volutová 2523, 150 00 Prague, Czech Republic
Corresponding author: Václav Ficaj (ficaj@fzp.czu.cz)

Key Points:

- A new physical wellbore model was constructed to track skin and wellbore storage effects.
- The model can be used for pumping tests in both steady-state and transient modes.
- Skin effect, wellbore storage modelling of various skin effects, and wellbore storage evaluations are enabled.

Abstract

Pumping tests were conducted on a completely unique physical well model to monitor the efficiency and aging rate of groundwater wells. In these tests, the main indicator of wellbore efficiency and functionality was the magnitude of the skin effect on the wellbore and its immediate surroundings. To study skin effects, a physical wellbore model was designed and constructed. Owing to the size of the model and number of observation probes, it is possible to monitor aquifer processes in detail according to the influence of the skin effect. Considering the appropriate placement of the observation probes, it was possible to follow the evolution of the piezometric height in the wellbore casing during the pumping test. The design of the physical model of a wellbore allows for the simulation of skin effects on the wellbore casing and wellbore aging processes, such as clogging of the wellbore and the surrounding aquifer.

1 Introduction

The basic solution of an transient radially symmetrical groundwater flow to an 'ideal wellbore' (i.e. a wellbore without additional resistances that does not consider the influence of wellbore volume on the pumping test) was published by C.V. Theis, 1935. The Theis-type curve method was used to evaluate the basic aquifer parameters of transmissivity and storativity. The Cooper-Jacob semilogarithmic method [Cooper-Jacob, 1946] is still used to evaluate the physical parameters of the aquifer. This method is based on a simplification of the Theis solution for later pumping test times, where a straight-line segment appears in the semi-logarithmic plot of the pumping test drawdown versus log time (see Figure 7). When solving the pumping test on a 'actual wellbore' versus the 'ideal wellbore' of the Theis solution, the influence of additional resistances and the wellbore volume on the pumping test progress must be considered. The effect of wellbore volume on the progress of the pumping test was addressed in [Papadopulos and Cooper, 1967] and again in an oil field by [Ramey, 1970]. The volume of water in the 'actual wellbore' affects the pumping test at the beginning of pumping and completely disappeared at later pumping times. The second parameter that significantly affects pumping tests on a 'actual wellbore' is the additional resistivity generated in the well and its immediate surroundings (skin effect). Many factors affect the skin, including physical, chemical, and biological processes. Additional resistances have been discussed in detail in [Kruseman, de Ridder, 2008], [Walton, 2007], and [Houben, Treskatis, 2007], among other studies. The concept of the skin effect was first introduced by [Hurst, 1949] and [van Everdingen, 1953], who defined the change in permeability caused by an infinitesimally thin region around the wellbore as either reducing permeability (positive skin effect) or increasing permeability (negative skin effect). [Van Everdingen, 1953] first expressed the drawdown caused by additional resistance to steady flow. In the petroleum field, [Agarwal, 1970] published a solution for the basic equation of steady flow to a wellbore, considering additional resistances (skin effect) and the effect of wellbore volume (wellbore storage) on the pumping test using dimensionless parameters. His solution has become the basis for deriving various methods for determining skin effects and wellbore storage, such as type curve methods [Earlougher, 1977], [Yeh, Chang, 2013], [Mashayekhizadeh, Ghazanfari, 2011], [Kuchuk, Kirwan, 1987], which are reported in [Bourdet, 2002], [Walton, 2007], [Kruseman, de Ridder, 2008], [Nowakovski, 1989], and other studies. Furthermore, [Kucuk and Brigham, 1979] addressed this issue. The magnitude of the additional resistance is directly proportional to the groundwater flow velocity through the affected area near the wellbore [Chen and Chang, 2002]. [Mathias and Butler, 2007] extended the solution of [Kucuk and Brigham, 1979] by introducing wellbore storativity and horizontal anisotropy. This method was solved in Laplace space. [Yang et. al., 2005] extended the solution of [van Everdingen and Hurst, 1949] by introducing a partially permeable wellbore. [Kahuda and Pech, 2020] and [Ficaj et. al., 2021] solved for additional resistances and wellbore storage from the early portion of the pumping test (portion before Cooper-Jacob straight-line). The proposed method is based on a solution published by Agarwal (1970) using a Laplace transform [Walton, 2008]. Algorithm 368 [Stehfest, 1970] is used to invert the Laplace transform.

The measurement and evaluation of the skin effect on wellbores are usually performed in 'actual wells' but are affected by inaccuracies in field measurements, which are caused by the heterogeneity of the hydrogeological environment and possible clogging of the aquifer near the well. Another factor that makes it impossible to evaluate the skin effect under real conditions is the absence of observation probes in the gravel pack of the wellbore or its vicinity. However, measurements on a physical model of the wellbore allow for the accurate evaluation of the skin effect under precisely defined and adjustable conditions.

A detailed simulation and evaluation of the skin effect in a laboratory model of a wellbore with similar characteristics have not yet been published. However, [Saleh et al., 1997] investigated the formation damage caused by mud in the case of horizontal wells. In this study, a small horizontal wellbore physical model was developed to simulate actual well damage. The contribution of this study is the simulation of the radial groundwater flow in a fully 3D physical wellbore model. Fully 3D models are less common because they are more challenging to handle and observe [Stoeckl L, Houben G, 2023]. However, they allow both an accurate simulation of real conditions and the ideal placement of observation piezometers to obtain sufficient data for evaluating the skin effect.

2 Materials and Methods

2.1 Physical laboratory wellbore

A physical laboratory model of groundwater flow was constructed to investigate the hydraulic parameters of groundwater wellbores and their changes with respect to the nature of groundwater aquifers, method of exploitation, and evolution of chemical and bacteriological characteristics. On a laboratory scale, the model is designed to maximise the input homogeneity of the hydraulic properties to allow experiments to test individual parameters and situations known from 'actual wellbores', where it is difficult to separate other influencing factors. A physical model was used to investigate the wellbore skin effect and the development and influence of wellbore clogging, including experimental testing of recovery measures.

The conceptual design of the laboratory physical model of groundwater flow in the vicinity of the wellbore reflects the required accuracy and geometric design to simulate a hydraulic condition referred to as a ‘circular island’ where the model area is cylindrical, at the edge of which a constant level boundary condition is simulated, thereby fixing the range of groundwater level depression. The assembly was designed to simulate both the phreatic and confined heads, where the position of the overpressure reservoir controlled the pressure. When simulating a confined level, it is necessary to overlay the model with an impermeable cap.

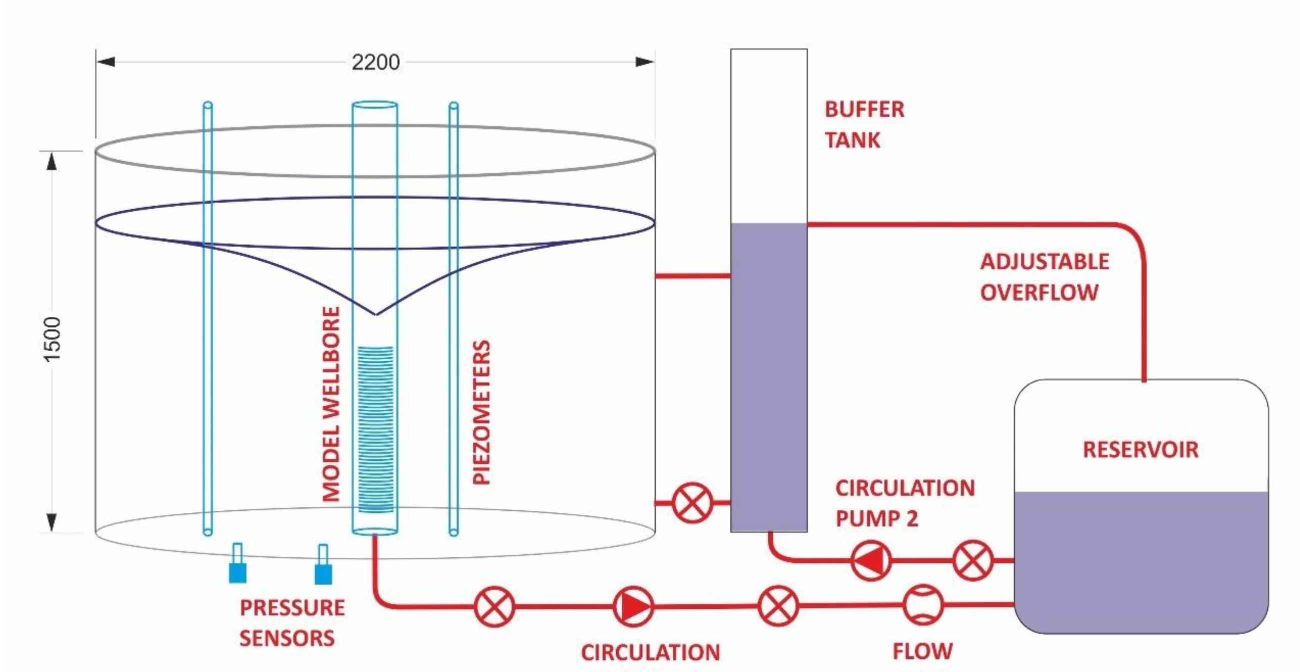

Figure 1 Scheme of the model, dimension [mm]

A wellbore was then located at the centre of the model, around which eight piezometers with automatic groundwater level pressure sensors were located radially. A centrifugal pump was installed in the centre of the borehole to regulate the output flow, which was measured using an inductive flow meter. Automatic data loggers recorded the flow rates and pressure sensor data at one-second intervals.

2.2 Construction details

2.2.1 Test tank

It is a single-skinned PE tank (Figure 2) with a total volume of 5.5 m3, a specific gravity of approximately 2.2 kg l-1. The base of the tank was a steel structure with a load capacity of up to 12 t. The bottom of the tank was perforated with a central DN50 outlet (for anchoring the simulated d = 175 mm wellbore screen) and eight secondary DN25 mm outlets (for connecting the pipeline to the observation probes). A perforated drainage pipe (d = 50 mm) was coiled around the inner perimeter of the tank to provide a uniform inflow of water to the periphery of the system.

2.2.2 Technical design specification

Single-skinned tank, flat bottom, without lid; steel support structure with a bottom liner and probe outlets.

- d = 2200 mm, h = 1500 mm
- Height of steel structure = 400 mm
- Total tank height = 1900 mm
- The supporting structure consists of an outer rim and inner ribs to fix the drainage pipe (eight pieces).
- Drainage pipe dimensions: d = 50 mm; l = 250 m.

2.2.2.1 Material used

- PE HWU
- Pipes and outlets of the tank: PE
- Supporting steel structure: steel class 11 with coating
- The PE used is UV stabilized

Figure 2. Top view of the test tank

2.2.2.2 Wellbore equipment

The wellbore was equipped with a wellbore casing (GWE PVC-U d195/10.0 (DN175)) with a socketed joint.

2.2.2.3 Porous material

The actual volume of the main tank was filled with a homogeneous sand PR13 (Provodínské písky, a.s.) fraction of 0.5/1 mm and laboratory-determined values of saturated hydraulic conductivity K = 1.9E-04 ms-1. The well gravel pack of 50 mm thickness consists of filtration gravel with a 2/5 mm fraction.

2.2.3 Buffer tank

The buffer tank was connected to the winding of a perforated pipe (d = 50 mm) and regulated at the outer edge of the main tank using a movable overflow.

2.2.4 Observation probes

The model contained 10 observation probes, 8 of which were located at the bottom of the main reservoir at various distances from the wellbore and routed through a PE d = 32 mm pipe. Point 9 was located at the bottom of the buffer tank, and point 10 was located directly in the wellbore. Piezoceramic sensors (0–160 mbar, 0.25%) were connected to the control unit via data cables. Table 1 lists the distances between each probe and the wellbore axis. Figure 3 shows the location of the observation probes.

Table 1. Observation probe positions

	Probe	r[m]	Note:
1	I	0.2	
2	II	0.1	
3	IV	0.05	
4	V	0.15	
5	VI	0.3	
6	VII	0.36	
7	VIII	0.6	
8	X	0.8	
9	tower		buffer tank
10	centre	0	wellbore

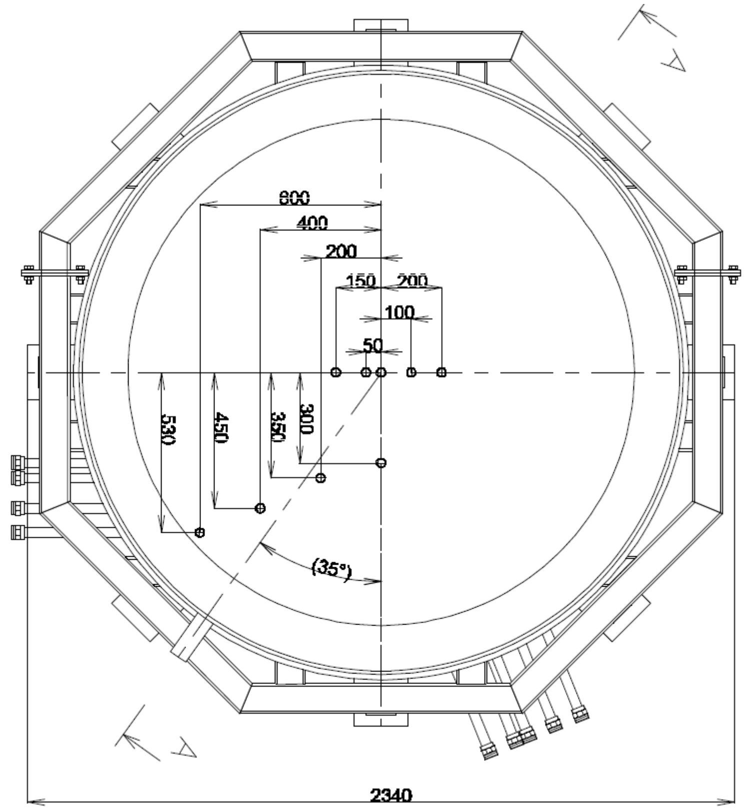

Figure 3. location of the observation probes

2.2.5 Circulation pump system and control

The model was equipped with a two Calpeda C 20E 230/400V 0.37 kW circulating pumps (Figure 4). The pumps provided water circulation between the physical model, water reservoir and buffer tank. Pump 1 transferred water from the wellbore at the centre of the physical model to the reservoir via an induction flow meter. Pump 2 transferred water from the reservoir to the peripheral section of the physical model via a column buffer tank.

PUMP 1: wellbore -> flow meter -> reservoir

PUMP 2: wellbore -> buffer tank

Figure 4. Placement of Calpeda C 20E 230V circulating pumps

The pumps were independently controlled by 230V/0.37kW frequency converters (Figure 6) and were connected via the control unit to the outputs of the pressure sensors of the wellbore and buffer tank and inductive flow meter. In manual mode, any setting is possible within the operating frequency. Range (30–50 Hz) or pumping capacity range (0–0.6 ls-1). In the automatic mode, two scenarios can be simulated:

A. Constant level in the wellbore

The frequency converter adjusts the pump rotation speed according to the set water level in the wellbore, with the pumped yield as the variable.

B. Constant yield from the wellbore

The frequency converter maintained the pump rotation speed at a constant level, and the variable value was the wellbore water level.

2.2.6 Data management and recording system

In this design, the data management and recording system is a module with a connected control display and data logger (Figures 5–6), which allows high frequency recordings of values (up to 1x / 0.1 s). The data are stored on a memory card and sent to the in parallel, using the GSM module for server storage. The system is based on the Raspberry Pi platform.

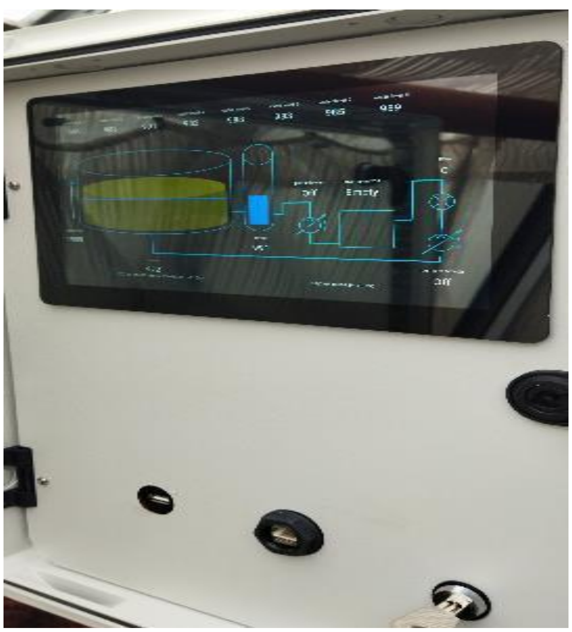

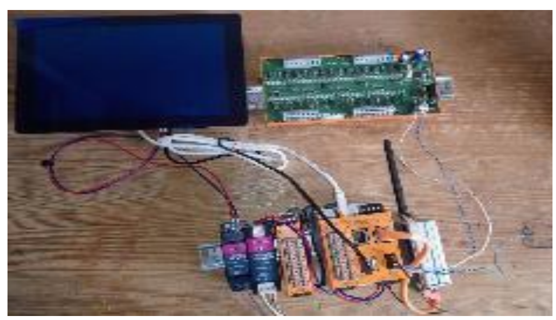

Figure 6. Control and recording module

Figure 5. Control panel

3 Data

3.1 Pumping tests

After constructing the model, a series of pumping tests were conducted to evaluate the functionality of the system. Having established all operational model components, we proceeded to test the model properties. Nine pumping tests were conducted to evaluate the skin effects, inhomogeneity, and anisotropy of the aquifer. Individual tests for three successive discharges and for three skin effect sizes were performed at 0.2, 0.3, and 0.4 ls-1. The purpose of these tests was to determine the properties of the model. The parameters investigated were aquifer storage S, aquifer transmissivity T and hydraulic conductivity K. Figures 8a–8c show the wellbore drawdown curves for different discharges. These drawdown plots were typical of homogeneous and isotropic aquifers. Typical sections of the drawdown process are clearly visible, namely, the first- and second-line segments (Figure 7). Furthermore, there was a gradual increase in the drawdown during the first few seconds. This is owing to the wellbore storage, which is high in the case of the model owing to the large wellbore diameter. The wellbore diameter is 0.175 m.

3.2 Evaluation of parameters

Figure 7 is a typical plot of a pumping test on a 'actual wellbore' (i.e., a wellbore, where we consider the effect of wellbore volume and additional resistances in the wellbore and its immediate surroundings (Agarwal). We can distinguish two line segments in the graph. The first straight line characterizes the initial section of the pumping test, where the wellbore volume and the additional resistances influence its course). The second-line segment was evaluated using the Cooper-Jacob approximation. In this part of the pumping test, the influence of wellbore volume on the pumping test data disappears.

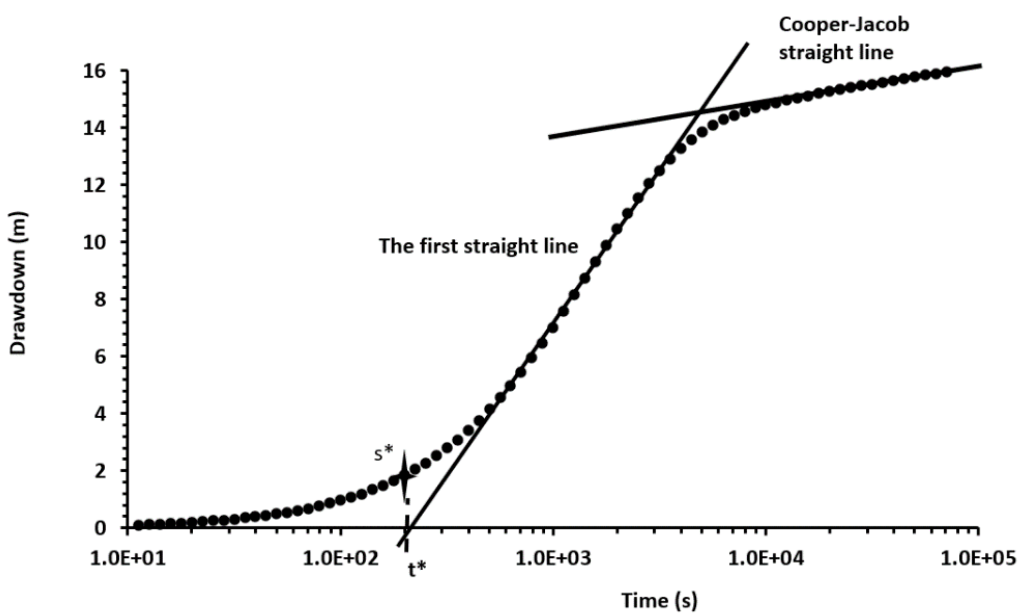

Figure 7. Diagram of a pumping test on a 'actual wellbore'

Twelve pumping tests were performed on the physical model. A total of 4 series of tests were performed. One series was performed without skin effect simulation and 3 series were performed with skin effect simulation. Each series was performed for 3 different pumping rates. the pumping rates were 0.2, 0.3 and 0.4 L/s. The resulting pumping tests with skin effect simulation are shown in Figures 8a, 8b and 8c.

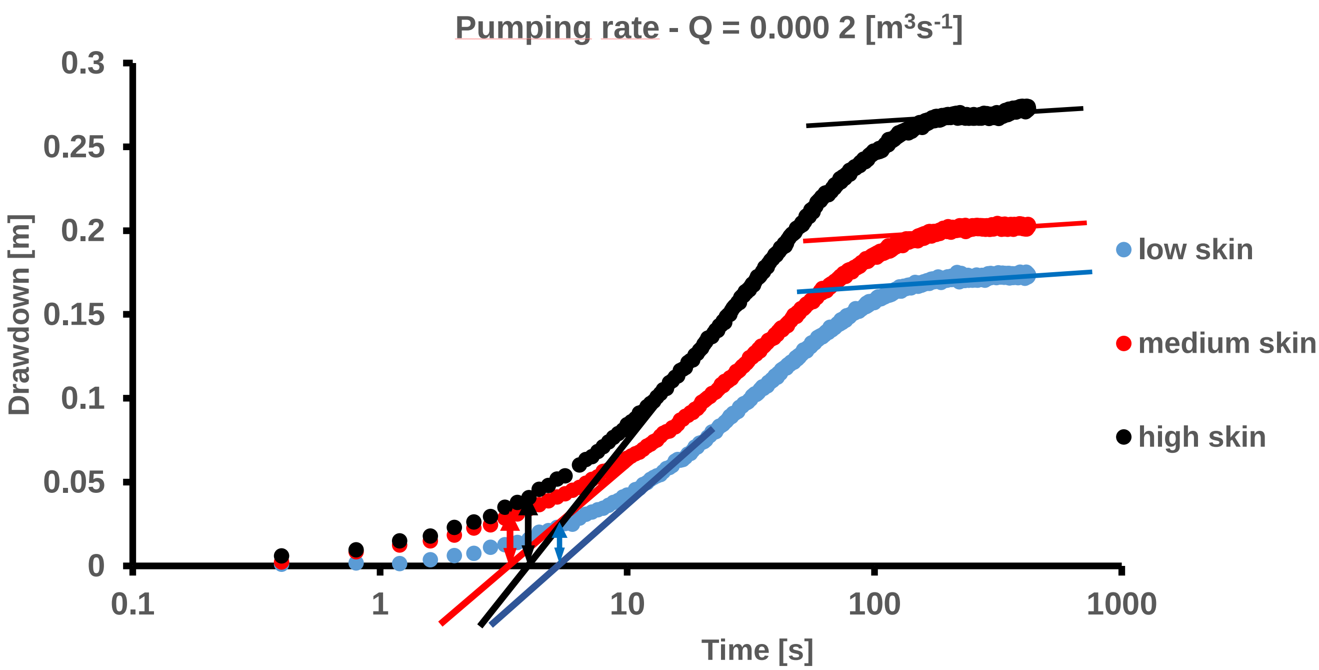

Figure 8a. Graph of pumping test on the physical model. Pumping rate: 0.0002 m^3s^{-1}.

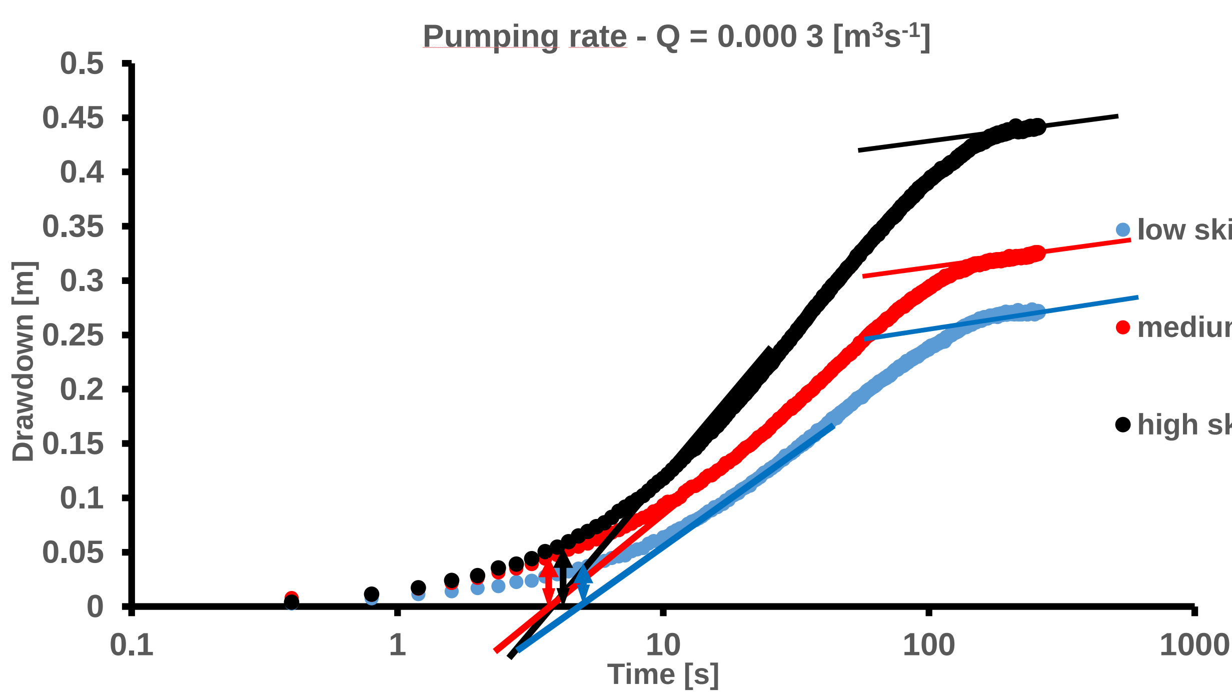

Figure 8b. Graph of pumping test on the physical model. Pumping rate: 0.0003 m^3s^{-1}.

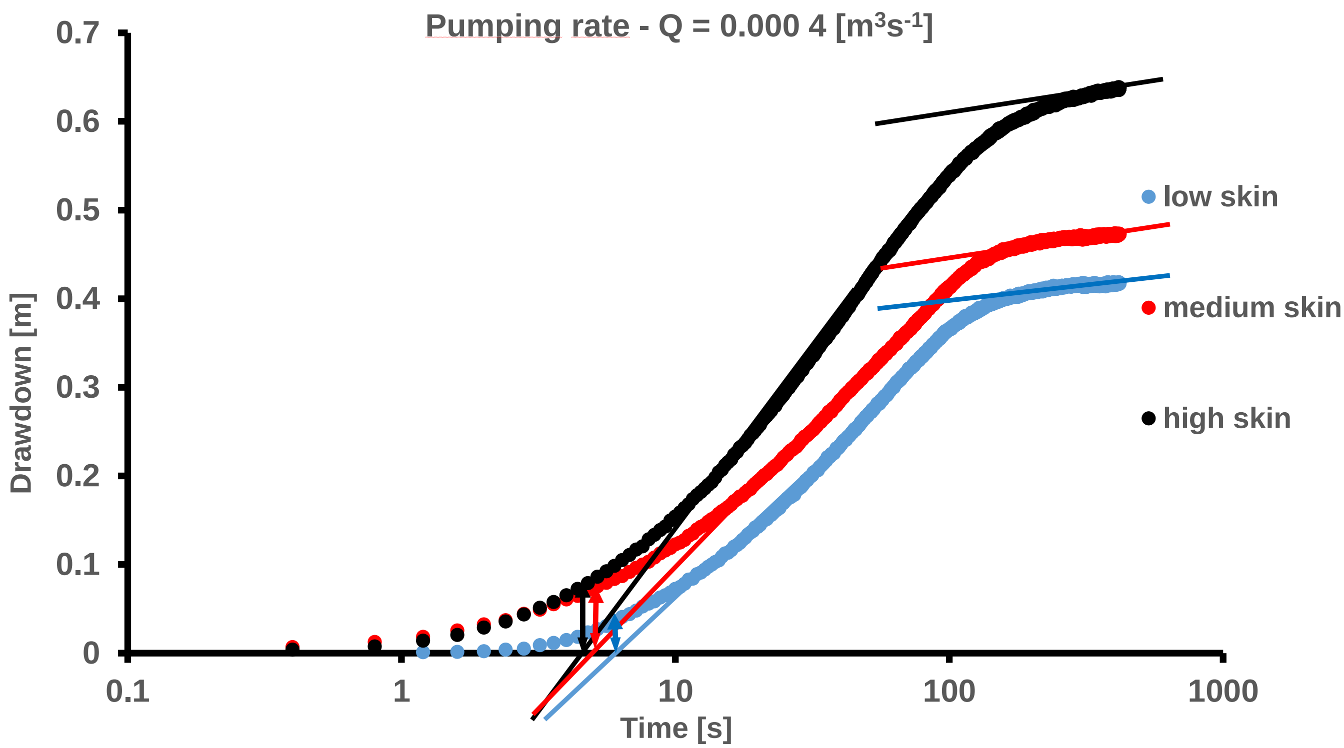

Figure 8c. Graph of pumping test on the physical model. Pumping rate: 0.0004 m^3s^{-1}.

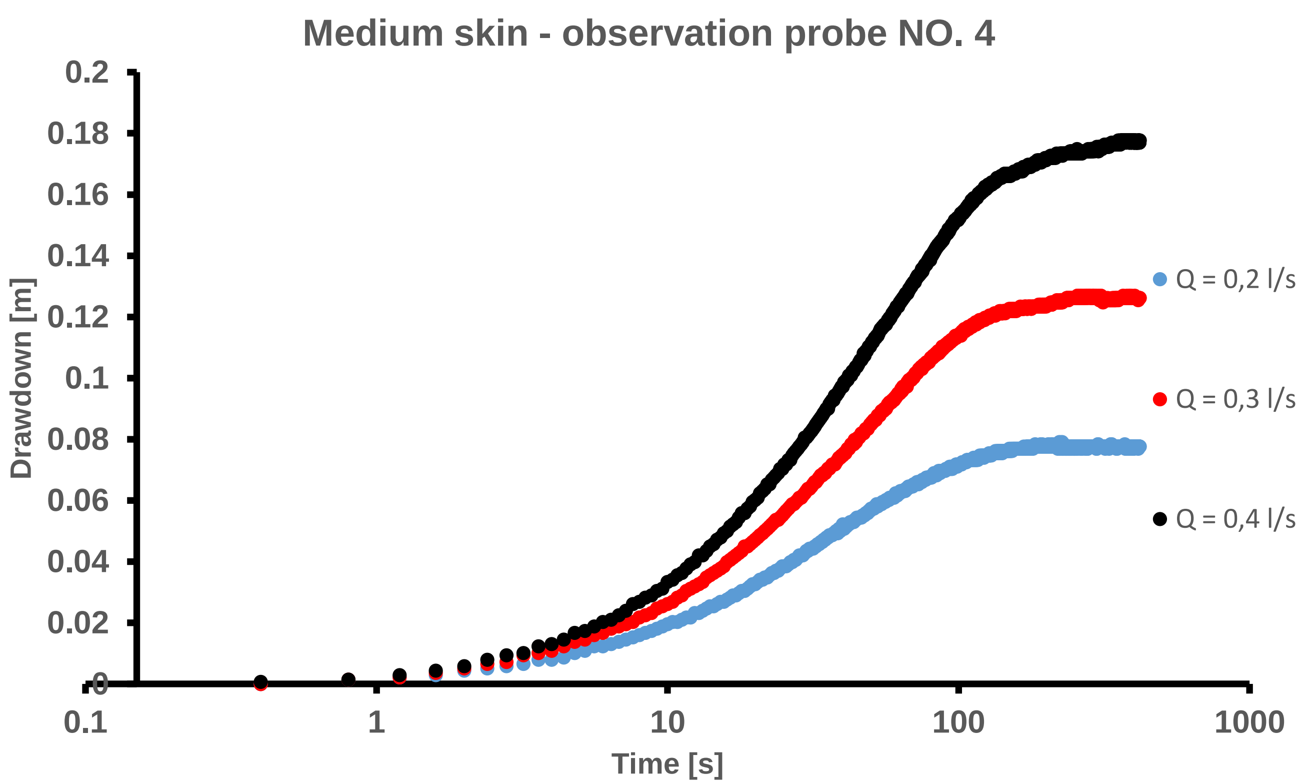

Figure 9. Graph of drawdown in observation probe number 4

3.2.1 Transmissivity

Transmissivity was evaluated using the Cooper-Jacob method [Horne, 1995]. The drawdown equation is as follows:

$$s_w = \frac{Q}{4\pi\, T} ln \frac{2.246\, Tt}{r_w^2 S} \qquad (1)$$

If we use the decadic logarithm after adjustment, we get the equation

$$s_w = \frac{0.183Q}{T} log \frac{2.246\, Tt}{r_w^2 S} \qquad (2)$$

where Q is the discharge pumped from the wellbore (m^3s^{-1}); T is the transmissivity of the aquifer (m^2s^{-1}); t is time (s), r_w is the wellbore radius (m), S is the storativity of the aquifer (-), s_w the drawdown in the wellbore (m).

For the two chosen times t_2 and t_1, we subtract the corresponding drawdowns s_2 and s_1 in the Cooper-Jacob section. Then, using Equation (2), we can write

$$\Delta s = s_2 - s_1 = \frac{0.183Q}{T} log \frac{t_2}{t_1} \qquad (3)$$

from Equation (3), we express the transmissivity

$$T = \frac{0.183Q}{i} \qquad (4)$$

where

$$i = \frac{s_2 - s_1}{log\ t_2 - log t_1} \qquad (5)$$

i is the slope of the Cooper-Jacob straight-line (see Figure 7).

3.2.2 Storativity

The aquifer storage was evaluated using a solution published by [Cooper and Jacob, 1946], as shown in Equation 6:

$$S = \frac{2.246 T t_0}{r_p^2} \qquad (6)$$

where t_0 is the intersection time of the extrapolated line of the observation probe (s), s = f (log t) with the log t axis (drawdown = 0) (s), r_p the distance of the observation probe from the axis of the pumped wellbore (m).

3.2.3 Skin factor

Two methods were used to calculate the skin factor of a 'actual wellbore'. The first calculation was based on the Cooper-Jacob equation for a 'actual wellbore' [Horne, 1990] (METHOD_1) and is given by Equation (7).

$$s_w = \frac{Q}{4\pi T}\left(ln\frac{2.246\,Tt}{r_w^2 S} + 2W\right) \qquad (7)$$

If we use the decadic logarithm after adjustment, we get Equation (8)

$$s_w = \frac{0.183Q}{T}\left(log\frac{2.246\,Tt}{r_w^2 S} + 2W\right) \qquad (8)$$

from Equation (8), we express the skin factor

$$W = \frac{1}{2}\left(\frac{s_w T}{0.183\,Q} - log\frac{2.246\,Tt_c}{r_w^2 S}\right) \qquad (9)$$

To evaluate the skin factor, a second method (METHOD_2) was used using part of the pumping test before reaching the Cooper-Jacob section (initial part). The derivation of this procedure is provided by [Kahuda, Pech, 2020]. The derived relationship has the following form:

$$W = \frac{1}{0.166}\left(\frac{2\,\pi\,Ts^*}{Q} - 0.1908\log\frac{C}{2\pi r_w^2 S} - 0.2681)\right) \qquad (10)$$

where for t* (is the time of intersection of the first line (see Figure 7) with the time axis) (s) and s* is the drawdown at this time (m); C is the unit wellbore volume factor defined by Ramey, 1970 (m^2) and can be expressed by Equation (11):

$$C = Q\frac{t_b}{s_b} \qquad (11)$$

s_b and t_b are the time and drawdown from the complete start of the pumping test, respectively, when all water is pumped from the wellbore's own volume (no water flows into the wellbore from the aquifer). This section takes a few seconds to minutes and depends on the wellbore radius and the amount of water pumped from the wellbore.

4 Results

Table 2 lists the parameters of the proposed model. For aquifer transmissivity, the average value was 0.003 m^2s^{-1}. The storage activity of the aquifer is 0.057. The resulting skin effect values were positive for all measurements. The values obtained by both methods are very similar. The resulting values and their percentage difference are shown in Table 2. The difference in results ranges from 0.7% to 8.7%. These results show that the model media acted homogeneously, as almost the same results were obtained, despite the fact that the two different calculation methods were used for three different discharges. The average aquifer hydraulic conductivity parameter K was 0.0029 on average. The aquifer storativity parameter S was 0.057 on average.

Table 2. Resultant parameters

Pumping test	**Q** (m^3s^{-1})	**skin**	**W** METHOD_ 1 (-)	**W** MEHOD_2 (-)	Difference between methods 1 and 2 (%)
1	0.0002	low	12,0786	12,6087	4,2
2	0.0002	medium	14,9046	15,4587	3,6
3	0.0002	high	21,4986	22,2681	3,5
4	0.0003	low	12,8601	11,9073	7,4
5	0.0003	medium	15,662	15,3122	2,2
6	0.0003	high	22,3471	22,5001	0,7
7	0.0004	low	13,2028	12,0475	8,7
8	0.0004	medium	14,8039	15,4490	4,2
9	0.0004	high	22,8782	21,9782	4

5 Discussion

5.1 Technical design of the physical wellbore model

The original design of the physical model was modified somewhat during its construction when it was necessary to respond to unexpected measurement complications. The main challenges are detailed below and were incorporated to improve device functionality and facilitate applicability in specific cases.

The limiting factor of the constructed physical model was its dimensions, which were adapted to the locations inside the laboratory. This is also related to the necessity of downscaling the problem, where the standard dimensions of the casing and wellbore gravel pack are maintained to investigate the additional resistances on a 'actual wellbore'.

In the case of the porous material used, some effort has been made to downscale the effective grain diameter while maintaining conductivity values on the order of e-3 or so, so that the drawdown was wellbore measurable under laboratory conditions. For this purpose, several mixtures of 0.5/1 mm sand fractions with quartz dust in different proportions were prepared, and their conductivities were measured independently in a soil laboratory. However, the mixtures produced by this process proved to be mechanically unsuitable, as the fine components leached out and temporary cracks formed after drying. Therefore, only the homogeneous PR13 fraction was used in the actual model.

In the limited space of the physical model, the structures of the observation probes also presented significant inhomogeneity, in which the eight probes could affect the actual groundwater flow and, thus, measurement accuracy. Therefore, holes (d=32 mm) were drilled into the bottom of the tank in the original design and connected to the pressure sensors through pipes. In practice, this measurement method has not been very successful because there appears to be a delay in the time of influence of the observation probes. The reason for this is unclear; however, we believe that it is a manifestation of hidden preferential groundwater flow paths. Therefore, 3 pcs of the standard piezometers (d=32 mm) were added to the model, and their measurements were primarily used to determine the hydraulic parameters of the porous medium. The circulation pumps were replaced with more powerful ones because the original configuration failed to achieve the equilibrium state of pumping and recharge at the simulated boundary condition.

5.2 Pumping tests and skin effect evaluation

Physical model measurements were used to evaluate the aquifer transmissivity, hydraulic conductivity, and aquifer storage parameters. To evaluate aquifer storativity, data obtained from three model pumping tests for different pumping rates were used for the physical model. Storativity was determined as the average of three observation probes 0.3, 0.6, and 0.8 meters from the wellbore centerline for all three pumping rates.

For the evaluation of the coefficient of additional resistances (skin factor), two methods were used from the pumping tests: the classical Cooper-Jacob method with the inclusion of the influence of additional resistances in the basic Cooper-Jacob equation using a dimensionless skin factor (METHOD_1); for the initial region of the pumping test (see Figure 7), a new method derived in [Kahuda, Pech 2020] (METHOD_2) was applied, which could be used when the Cooper-Jacob section was not reached. To derive this method, the solution of the basic partial differential equation describing the transient radially symmetric flow into a borehole [Agarwal, 1970] was used. A Laplace transform [Walton, 2008] was also used for this solution. The real-space solution was obtained using the Stehfest algorithm 368 [Stehfest, 1970]. The Stehfest algorithm is commonly used for numerical inversion of the Laplace transform in the petroleum and groundwater flow domains. The new method is applicable to the initial part of the pumping test before reaching the Cooper-Jacob section. The derivation of this method has been described in detail by [Kahuda and Pech, 2020]. The results of the skin factor calculations using both methods are listed in Table 2. From the skin factor calculations using both methods, METHOD_1 and METHOD_2, and a comparison of the values from the three pumping tests again showed good agreement. In the calculations, the skin factor exhibited a negative value because the coarser gravel was used as backfill in the physical model, causing a reduction in the hydraulic gradient in the backfill area. This results in 'negative' additional resistances. Once the physical model has been commissioned and debugged, further measurements can be taken. For example, it will be possible to monitor and evaluate changes in additional resistivity at the well itself and its immediate surroundings, simulate aquifer heterogeneity, monitor the effect of boundary conditions on the pumping tests, and simulate the flow to the well with a free surface.

6 Conclusions

The main purpose of this study was to test the entire system of a physical wellbore model. As expected, the results showed that the physical model worked correctly. The ability to change and evaluate the magnitude of the skin effect on a wellbore was confirmed in this study.

The largest contribution of this model is its ability to simulate the homogeneity, inhomogeneity, isotropy, and anisotropy of an aquifer. However, the constructed wellbore model has broad applications for detailed hydraulic testing. The main capabilities of the model are as follows.

- Simulating radial groundwater inflow for pumped wellbore measurement of depressional groundwater flow curves and calibration of mathematical models
- Testing porous sedimentary materials for hydraulic properties
- Monitoring the development of wellbore clogging
- Measuring wellbore oxidation–reduction characteristics
- Simulating unconfined and confined aquifers
- Testing usable yields in wellbores
- Testing recovery measures

The next stage of the model research will involve simulating various additional resistances at the wellbore. These evaluations were used to verify the validity of the proposed method to determine additional resistances from the initial section of the pumping test.

Acknowledgments

The project was supported by the IGA Faculty of Environmental Sciences CZU Prague 'An artificial intelligence-based model for finding the storativity parameter of an aquifer, Václav Ficaj – No. 2022B0019'. Faculty of Environmental Sciences, Czech University of Life Sciences Prague, Kamýcká 129, Praha – Suchdol, 165 00, Czech Republic and by Technology Agency of the Czech Republic, grant number SS01020224 'Small groundwater rehabilitation apparatus'.

Open Research

Data from our own measurements were used in the creation of this manuscript. The dataset contains 6 pumping tests presented in manuscript. These data are freely available on the website: https://home.czu.cz/pech/wrr-2023wr036150

References

Theis, C.V. (1935), The relation between the lowering of the piezometric surface and the rate and duration of discharge of a well using ground-water storage. Trans. Am. Geophys. Union, 16, 519–524, doi:10.1029/TR016i002p00519.

Cooper, H.H.; Jacob, C.E. (1946), A generalized graphical method for evaluating formation constants and summarizing well-field history. Trans. Am. Geophys. Union, 27, 526–534, doi:10.1029/TR027i004p00526

Saleh, S.T.; Rustam, R.W.; El-Rabaa; Islam, M.R. (1997), Formation damage study with a horizontal wellbore model. Journal of Petroleum Science and Engineering, Volume 17, Issues 1–2

Papadopulos, I.S.; Cooper, H.H. (1967), Drawdown in a well of large diameter. Water Resour. Res. 3, 241–244, doi:10.1029/WR003i001p00241.

Wattenbarger, R.A.; Ramey, H.J. (1970), An investigation of wellbore storage and skin effect in unsteady liquid flow: II. Finite difference treatment. Soc. Pet. Eng. J. 10, 291–297, doi:10.2118/2467-pa

Kuraz, M., Mayer, P., Havlicek, V. *et al.* (2013), Domain decomposition adaptivity for the Richards equation model. *Computing* **95** (Suppl 1), 501–519, doi: 10.1007/s00607-012-0279-8

Van Everdingen, A.F. (1953), The skin effect and its influence on the productive capacity of a well. J. Pet. Technol. 5, 171–176, doi:10.2118/203-G

Van Everdingen, A.F.; Hurst, W. (1949), The application of the Laplace transformation to flow problems in reservoirs. J. Pet. Technol. 1, 305–324, doi:10.2118/949305-G.

Agarwal, R.G.; Al-Hussainy, R.; Ramey, H.J. (1970), An investigation of wellbore storage and skin effect in unsteady liquid flow: I. Analytical treatment. Soc. Pet. Eng. J. 10, 279–291, doi:10.2118/2466-PA.

Kucuk, F.; Brigham, W.E. (1979), Transient flow in elliptical systems. Society of Petroleum Engineers Journal 19, 401-410. DOI: 10.2118/7488-PA.

Chen, Ch.S.; Chang, Ch.Ch. (2006), Theoretical evaluation of non-uniform skin effect on aquifer response under constant rate pumping. Journal of Hydrology 317,190-201. https://doi.org/10.1016/j.jhydrol.2005.05.017

Mathias, S.A.; Butler, A.P. (2007), Flow to a finite diameter well in a horizontally anisotropic aquifer with wellbore storage. Water Resources Research 43, 1-6. DOI: 10.1029/2006WR005839

Yang, S.Y.; Yeh, H.D. (2005), Laplace-domain solutions for radial two-zone flow equations under the conditions of constant-head and partially penetrating well. J. Hydraul. Eng. ASCE 131, 209–216, doi:10.1061/(ASCE)0733-9429(2005)131:3(209).

Garcia, L.A.; Shigidi, A. (2006), Using neural networks for parameter estimation in ground water. Journal of Hydrology 318 (1-4), 215-231

Kahuda, D.; Pech, P. (2020), A new method for evaluation of well rehabilitation from the early-portion of the pumping test. Water, 12, 744.

Ficaj, V.; Pech, P.; Kahuda, D. (2021), Software for Evaluating Pumping Tests on Real Wells. Appl. Sci, 11, 3182

Kukačka, J.: Pech, P.: Kahuda, D.: Ficaj, V. (2022), INV-FLOW: New Possibilities to Evaluate the Technical Condition and Function of Extraction Wells. Water, 14. 10.3390/w14132005.

Ramey Jr., H.H. (1970) Short-time well test data interpretation in the presence of skin effect and wellbore storage. Journal of Petroleum Technology, 22, 97-104.

Horne, R.N. (1990) Modern well test analysis: a computer aided approach, 4th. ed.; Petroway, Inc.: Ed. Palo Alto, US,; pp. 185 ISBN -0-9626992-09.

STOECKL, L a G HOUBEN. (2023) How to conduct variable-density sand tank experiments: practical hints and tips. *Hydrogeology Journal: Official Journal of the International Association of Hydrogeologists* [online]. 1-18 [cit. 2023-07-27]. ISSN 14312174. Dostupné z: doi:10.1007/s10040-023-02635-4

Bourdet, D. (2002) Well test analysis: The use of advanced interpretation models. Handb. Pet. Explor. Prod. 3, 1–426.

Watlton, W.C. (2007) Aquifer Test Modeling, 1st ed.; CRC Press: Boca Ralton, FL, USA, p. 240, ISBN-13: 978-1-4200-4292-4.

Kruseman, G.P.; de Ridder, N.A. (2008) Analysis and Evaluation of Pumping Test Data, 2nd ed.; IILRI: Wageningen, The Netherlands, pp. 1–372.

Earlougher, R.C., Jr. (1977) Advances in well test analysis. Monogr. Ser. Soc. Pet. Eng. AIME, 5, 264

Yeh, H.D.; Chang, Y.C. (2013) Recent advances in modeling of well hydraulics. Adv. Water Resour. 51, 27–51.

Mashayekhizadeh, M.D.; Ghazanfari, M.H. (2011) The application of numerical Laplace inversion methods for type curve development in well testing: A comparative study. Pet. Sci. Technol. 29, 695–707

Kuchuk, F.J.; Kirwan, P.A. (1987) New skin and wellbore storage type curves for partially penetrated wells. SPE Eval., 2, 546–554

Gringarten, A.C.; Bourdet, D.P.; Landel, P.A.; Kniazeff, V.J. (1979) A comparison between different skin and wellbore storage type-curves for early–time transient analysis. Soc. Pet. Eng. SPE Ann. Technol. C Exh. 1–16.

Stehfest, H. (1970) Algorithm 368: Numerical inversion of Laplace transforms. Commun. ACM, 13, 47–49.

Houben, G.; Treskatis, C. Water Well Rehabilitation and Reconstruction, 3rd ed.; McGraw Hill Professional: Two Penn Plaza, NY, USA, 2007; ISBN 0-07-148651-8.

Novakowski, K.S. A Composite analytical model for analysis of pumping tests affected by well bore storage and finite thickness skin. Water Resour. Res. 1989, 25, 1937–1946.